N-terminal transmembrane domain of SUR1 controls gating of Kir6.2 by modulating channel sensitivity to PIP_2

Emily B. Pratt, Paul Tewson, Cathrin E. Bruederle, William R. Skach, and Show-Ling Shyng

Department of Biochemistry and Molecular Biology, Oregon Health and Science University, Portland, OR 97239

Functional integrity of pancreatic adenosine triphosphate (ATP)-sensitive potassium (K_{ATP}) channels depends on the interactions between the pore-forming potassium channel subunit Kir6.2 and the regulatory subunit sulfonylurea receptor 1 (SUR1). Previous studies have shown that the N-terminal transmembrane domain of SUR1 (TMD0) interacts with Kir6.2 and is sufficient to confer high intrinsic open probability (P_o) and bursting patterns of activity observed in full-length K_{ATP} channels. However, the nature of TMD0–Kir6.2 interactions that underlie gating modulation is not well understood. Using two previously described disease-causing mutations in TMD0 (R74W and E128K), we performed amino acid substitutions to study the structural roles of these residues in K_{ATP} channel function in the context of full-length SUR1 as well as TMD0. Our results revealed that although R74W and E128K in full-length SUR1 both decrease surface channel expression and reduce channel sensitivity to ATP inhibition, they arrive there via distinct mechanisms. Mutation of R74 uniformly reduced TMD0 protein levels, suggesting that R74 is necessary for stability of TMD0. In contrast, E128 mutations retained TMD0 protein levels but reduced functional coupling between TMD0 and Kir6.2 in mini-K_{ATP} channels formed by TMD0 and Kir6.2. Importantly, E128K full-length channels, despite having a greatly reduced P_o, exhibit little response to phosphatidylinositol 4,5-bisphosphate (PIP_2) stimulation. This is reminiscent of Kir6.2 channel behavior in the absence of SUR1 and suggests that TMD0 controls Kir6.2 gating by modulating Kir6.2 interactions with PIP_2. Further supporting this notion, the E128W mutation in full-length channels resulted in channel inactivation that was prevented or reversed by exogenous PIP_2. These results identify a critical determinant in TMD0 that controls Kir6.2 gating by controlling channel sensitivity to PIP_2. Moreover, they uncover a novel mechanism of K_{ATP} channel inactivation involving aberrant functional coupling between SUR1 and Kir6.2.

The Journal of General Physiology

INTRODUCTION

The pancreatic β cell ATP-sensitive potassium (K_{ATP}) channel is a member of the inwardly rectifying potassium (Kir) channel family (Inagaki et al., 1995). It plays a key role in regulating insulin secretion by coupling cell metabolism to cell excitability (Aguilar-Bryan and Bryan, 1999; Nichols, 2006). The channel is a hetero-octamer composed of two different subunit types (Clement et al., 1997; Inagaki et al., 1997; Shyng et al., 1997). Four Kir6.2 subunits line the conduction pathway and are similar in topology and sequence to other members of the Kir channel family. ATP and phosphatidylinositol 4,5-bisphosphate (PIP_2) interact with Kir6.2 to inhibit or stimulate channel activity, respectively (Tucker et al., 1997; Baukrowitz et al., 1998; Shyng et al., 1998). Surrounding Kir6.2 are four sulfonylurea receptor 1 (SUR1) subunits, which are required for K_{ATP} channel trafficking and function. SUR1 is a member of the ATP-binding cassette transporter superfamily and contains the canonical ATP-binding cassette transporter core domain (two six-spanning transmembrane domains [TMDs] and two cytoplasmic nucleotide-binding folds) plus a unique five-spanning N-terminal TMD (TMD0) and a large cytosolic linker (L0) (see Fig. 1 A) (Aguilar-Bryan et al., 1995; Tusnády et al., 1997; Conti et al., 2001). SUR1 imparts K_{ATP} channels with sensitivities to MgADP stimulation and to pharmacological agents such as sulfonylureas and diazoxide (Nichols et al., 1996; Gribble et al., 1997). In addition, SUR1 modifies the properties of K_{ATP} channels by increasing the open probability (P_o) of Kir6.2 and making the channel more sensitive to ATP inhibition (Tucker et al., 1997; Babenko et al., 1999; Enkvetchakul et al., 2000). Despite advances in our understanding of the distinctive roles of SUR1 and Kir6.2 in K_{ATP} function, significant knowledge gaps remain with regard to the mechanisms of coupling between SUR1 and Kir6.2 that give rise to the gating properties of K_{ATP} channels.

K_{ATP} channel subunits can be manipulated to create unnatural yet useful channel variants to study channel structure–function relationships. Both Kir6.2 and SUR1 have a tripeptide ER-retention motif RKR that becomes shielded only upon proper formation of K_{ATP} quaternary

Correspondence to Show-Ling Shyng: shyngs@ohsu.edu

Abbreviations used in this paper: K_{ATP}, ATP-sensitive potassium; PIP_2, phosphatidylinositol 4,5-bisphosphate; SUR1, sulfonylurea receptor 1; TMD, transmembrane domain; WT, wild type.

The Rockefeller University Press $30.00
J. Gen. Physiol. Vol. 137 No. 3 299–314
www.jgp.org/cgi/doi/10.1085/jgp.201010557

structure (Zerangue et al., 1999). Deletion of the last 36 amino acids of Kir6.2 (Kir6.2ΔC36) removes its RKR motif and leads to surface expression of homotetrameric Kir6.2 channels in the absence of SUR1 (Tucker et al., 1997; Zerangue et al., 1999). These channels differ from wild-type (WT) SUR1-Kir6.2 channels in several respects (Tucker et al., 1997; Babenko et al., 1999; Enkvetchakul et al., 2000; Babenko and Bryan, 2003; Chan et al., 2003). First, although they are sensitive to ATP inhibition, the half-maximal inhibition concentration (IC_{50}) is ~10-fold higher than WT channels (Tucker et al., 1997). Second, they exhibit a markedly reduced intrinsic P_o, i.e., spontaneous activity in the absence of nucleotides in isolated membrane patches, compared with WT channels (P_o, ~0.1 vs. ~0.6 for WT). In addition, they have altered single-channel kinetics with brief openings separated by relatively long periods of closure, in contrast to WT channels that demonstrate bursts of activity with fast open and close events separated by longer closed intervals. Interestingly, the coexpression of Kir6.2ΔC36 with TMD0 results in "mini-K_{ATP} channels" with bursting behavior and intrinsic P_o that are similar to WT channels. However, ATP sensitivity of mini-K_{ATP} channels remains lower than that of WT; in fact, it is even lower than that of Kir6.2ΔC36 channels. Mini-K_{ATP} channels also lack response to MgADP stimulation or pharmacological regulation (Babenko and Bryan, 2003; Chan et al., 2003). Thus, TMD0 is sufficient to confer WT channels' bursting properties and high P_o, but the portions of SUR1 responsible for increased ATP sensitivity and other SUR1-endowed gating properties lie outside TMD0. The mechanism whereby TMD0 modulates the gating pattern of Kir6.2 has not been determined, although it has been proposed that intramembrane interactions reposition the Kir6.2 outer helix to achieve the effects (Babenko and Bryan, 2003).

Phosphoinositides, and in particular PIP_2, are key determinants of K_{ATP} channels' intrinsic P_o. Current data suggests that PIP_2 interacts with positively charged residues in the N- and C-terminal cytoplasmic domains of Kir6.2 near the lipid–cytoplasm interface to stabilize channel opening (Shyng et al., 2000; Cukras et al., 2002a,b; Haider et al., 2007). Activation of K_{ATP} channels by PIP_2 leads to a concomitant decrease in channel inhibition by ATP (Baukrowitz et al., 1998; Shyng and Nichols, 1998), which binds to a pocket formed by residues from the N- and C-terminal cytoplasmic domains of two adjacent Kir6.2 subunits (Antcliff et al., 2005). Although ATP and PIP_2 may interact with overlapping residues, they are not thought to be competitive ligands (Antcliff et al., 2005; Haider et al., 2007; Stansfeld et al., 2009). Rather, PIP_2 decreases the apparent channel sensitivity to ATP inhibition via allosteric effects. To date, most mutagenesis and modeling studies addressing the mechanism of PIP_2 regulation have focused on the Kir6.2 subunit. However, it has been well documented that SUR1 increases Kir6.2 response to PIP_2 (Baukrowitz et al., 1998; Enkvetchakul et al., 2000). Thus, how SUR1 modulates channel response to PIP_2 is an important question yet to be resolved.

Mutations in SUR1 or Kir6.2 that cause loss of K_{ATP} channel activity or expression result in congenital hyperinsulinism, whereas gain-of-function mutations cause neonatal diabetes (Ashcroft, 2005). Recently, we reported that two mutations (R74W and E128K) in the TMD0 domain of SUR1 identified in congenital hyperinsulinism cause loss of channel function by preventing channel trafficking to the cell surface. We showed that the trafficking defects can be overcome by treating cells with sulfonylureas (Yan et al., 2004, 2006, 2007), and upon rescue to the cell surface, mutant channels reveal gating defects expected to cause the opposite disease, neonatal diabetes (Pratt et al., 2009). The R74W- and E128K-mutant channels exhibit reduced channel sensitivity to ATP inhibition. However, unlike most ATP-insensitive mutants in which an increased P_o underlies the reduction in apparent ATP sensitivity by allosteric effects, the R74W and E128K mutants display decreased P_o (Pratt et al., 2009). These alterations resemble differences between WT and Kir6.2ΔC36 channels (Enkvetchakul et al., 2000) and suggest that R74 and E128 may be involved in TMD0–Kir6.2 interactions. In this study, we systematically replaced residues 74 and 128 with other amino acids (referred to as R74X and E128X) in full-length and mini-K_{ATP} channels to probe their structural and functional roles in the coupling of TMD0 to Kir6.2. We show that R74W reduces the stability of TMD0 protein and thus physical coupling between TMD0 and Kir6.2. In contrast, E128K disrupts functional coupling between TMD0 and Kir6.2 by abrogating the effects of SUR1 on channel response to PIP_2. Moreover, the mutation E128W leads to spontaneous current inactivation that can be prevented or reversed by PIP_2. The findings on the E128 mutations provide novel insight into the mechanism by which TMD0 of SUR1 modulates Kir6.2 gating. In Kir channels, PIP_2 plays a central role in determining channel activity (Hilgemann et al., 2001; Yi et al., 2001), and diverse modulators affect Kir channel activity via PIP_2 interactions (Baukrowitz et al., 1998; Shyng and Nichols, 1998; Fan and Makielski, 1999; Liou et al., 1999; Du et al., 2004). We propose that TMD0 confers intrinsic gating properties of K_{ATP} channels by modulating interactions between Kir6.2 and PIP_2.

MATERIALS AND METHODS

Molecular biology

Rat Kir6.2 cDNA constructs including the full-length WT subunit and a truncation mutant lacking the C-terminal 36 amino acids (Kir6.2ΔC36) are in pCDNAI/Amp plasmid (Lin et al., 2008). Hamster SUR1 constructs are in pECE and include full-length

subunits with an N terminus FLAG epitope (DYKDDDDK) (fSUR1) or the first TMD only (amino acids 1–198) with (fTMD0) or without (TMD0) the FLAG epitope. The FLAG epitope does not change biochemical or functional properties of the channel (Cartier et al., 2001). Site-directed mutagenesis was performed using the QuikChange mutagenesis kit (Agilent Technologies), and mutations were confirmed by direct sequencing.

Immunoblotting

COSm6 cells were maintained in DMEM with 10% FBS and 1% penicillin/streptomycin. Cells at ∼70% confluence on 35-mm dishes were transfected with 0.6 µg fSUR1 and 0.4 µg Kir6.2 (or 1 µg fTMD0 and 1 µg Kir6.2ΔC36; the amount of cDNA was adjusted to maintain a 1:1 molar ratio of SUR1 to Kir6.2 plasmids) using FuGene 6 (Roche). Cells were processed 48–72 h after transfection and, where indicated, 12–18 h after sulfonylurea treatment (300 µM tolbutamide; Sigma-Aldrich) (Yan et al., 2004, 2007). Cells were lysed in a buffer containing 20 mM HEPES, pH 7.0, 5 mM EDTA, 150 mM NaCl, and 1% Triton-X with Complete Protease Inhibitor Cocktail Tablets (Roche). Protein concentrations were determined using a Lowry assay (Bio-Rad Laboratories). An equal amount of protein from each sample was separated by SDS/PAGE, transferred to nitrocellulose membrane, analyzed by mouse M2 anti-FLAG antibody (Sigma-Aldrich) or rabbit anti-SUR1 generated against the C-terminal peptide (KDSVFASFVRADK) (Yan et al., 2007) followed by horseradish peroxidase–conjugated anti–mouse or anti–rabbit secondary antibodies (GE Healthcare), and visualized by chemiluminescence (Super Signal West Femto; Thermo Fisher Scientific). Densitometry was performed using ImageJ (National Institutes of Health).

Chemiluminescence assays

48 h after transfection, cells in 35-mm dishes were fixed with 2% paraformaldehyde for 30 min, preblocked in PBS/0.5% BSA for 30 min, incubated in M2 anti-FLAG antibody (10 µg/ml) for 1 h, washed four times for 30 min in PBS/0.5% BSA, incubated in horseradish peroxidase–conjugated anti–mouse antibodies for 20 min, and washed again four times for 30 min in PBS/0.5% BSA. Chemiluminescence was quantified using a luminometer (TD-20/20; Turner Designs) after a 10-s incubation in luminol solution (Power Signal ELISA Femto; Thermo Fisher Scientific). Results of each experiment are the average of two 35-mm dishes, and each data point shown in the figures is the average of at least three experiments.

Immunofluorescence staining

COSm6 cells were cotransfected with WT or mutant fTMD0 and Kir6.2ΔC36. After 24 h, cells were plated onto glass coverslips, grown for 24 h, and incubated with M2 anti-FLAG antibody (10 µg/ml OptiMEM containing 0.1% BSA) for 1 h at 4°C to label surface channels. Cells were then washed with ice-cold PBS, fixed with cold (−20°C) methanol for 10 min, and incubated with Alexa Fluor 488 goat anti–mouse secondary antibody (Invitrogen) for 45 min at room temperature. After three washes with PBS, cells were mounted and viewed with a three-spectral confocal microscope (LSM710; Carl Zeiss, Inc.) and a 63 × 1.4–NA objective (Carl Zeiss, Inc.).

Patch clamp recordings

Voltage clamp recordings from inside-out patches of transfected COSm6 cells were performed using an Axopatch 1D amplifier and pClamp9 acquisition software (Axon Instruments, Inc.) (Yan et al., 2004). For macroscopic recordings, micropipettes were pulled from non-heparinized Kimble glass (Thermo Fisher Scientific) on a horizontal puller (Sutter Instrument Co.) and had resistances of ∼1.5–2.0 MΩ. Micropipettes for single-channel recordings were pulled from either non-heparinized Kimble glass or borosilicate electrodes (Sutter Instrument Co.), coated with Sylgard-148 (Sigma-Aldrich), polished by microforge, and had resistances of ∼2–6 MΩ. The bath and pipette solution (Kint) was: 140 mM KCl, 10 mM K-HEPES, and 1 mM K-EGTA, pH 7.4. In all experiments (except those for Fig. 6), 1 mM EDTA was added to Kint (Kint/EDTA) to prevent channel rundown (Lin et al., 2003). All currents were measured at a membrane potential of −50 mV (+50-mV pipette potential) at room temperature, and inward currents are shown as upward deflections in all figures. When recording from cells expressing mutant channels with very little basal surface expression, the cells were pretreated with 300 µM tolbutamide overnight to augment expression.

Data analysis

Data are presented as means ± SEM. ATP inhibition dose–response data were fit with the Hill function ($I_{rel} = 1/(1 + ([ATP]/IC_{50})^H)$). I_{rel} is the current relative to maximal current in nucleotide-free Kint/EDTA solution, IC_{50} is the concentration of ATP that causes half-maximal inhibition, and H is the Hill coefficient. Statistical analysis was performed using independent two-population, two-tailed Student's *t* test, with $P < 0.05$ considered statistically significant. Single-channel P_o analysis was performed using the pCLAMP9 automated channel event detector. If a decrease in single-channel activity was noted, only activity recorded within the first 60 s of patch excision was used for analysis.

Online supplemental material

Fig. S1 shows the surface expression of R74X and E128X full-length K_{ATP} channels, as quantified by chemiluminescence after overnight pretreatment with 300 µM tolbutamide to rescue channel trafficking. Fig. S2 includes a protein sequence alignment performed by PRALINE (Simossis and Heringa, 2005) of TMD0 of SUR1 for human, hamster, dog, and zebrafish, and human SUR2. Additionally, predictions of how mutations at R74 might affect TMD0 topology calculated by TOPCONS prediction software (Bernsel et al., 2009) are shown. Figs. S1 and S2 are available at http://www.jgp.org/cgi/content/full/jgp.201010557/DC1.

RESULTS

In full-length K_{ATP} channels, R74 is sensitive to substitution by noncharge-conserving amino acids

COSm6 cells were transiently transfected with WT Kir6.2 along with WT or mutant SUR1, with an extracellular N-terminal FLAG epitope (fSUR1). Nine amino acids with diverse side chain properties (Chothia, 1976; Kyte and Doolittle, 1982) were swapped for arginine 74 of SUR1. 48 h later, chemiluminescence assays were performed (refer to Materials and methods), such that antibody directed against the FLAG epitope was detected using luminol reacting with horseradish peroxidase–conjugated secondary antibody. Because luminescence produced by this reaction is proportional to expression of K_{ATP} channels on the cell surface, quantification is possible (Margeta-Mitrovic et al., 2000; Taschenberger et al., 2002). Surface expression for every R74X-mutant tested, except the charge-conserving R74K mutation, was significantly reduced to <40% of WT (Fig. 1 B). Surface expression quantified by chemiluminescence assays was confirmed by Western blot experiments. SUR1 has

two N-linked glycosylation sites (at residues N10 and N1050) that are core glycosylated in the ER and acquire a complex carbohydrate during transit through the Golgi (Raab-Graham et al., 1999). K_{ATP} channel trafficking can therefore be monitored by the relative abundance of core- and complex-glycosylated SUR1. Complex-glycosylated SUR1 serves as a proxy measure of surface expression, although some fraction of "mature" protein may reflect channels in transit from Golgi to the plasma membrane and endosomal trafficking. Fig. 1 C (top) shows representative immunoblots using anti-SUR1 antibody. R74K, which had surface expression at 74 ± 4% of WT by chemiluminescence (Fig. 1 B), showed both upper and lower glycosylation bands. In contrast, R74A and R74Y (2 ± 1 and 4 ± 2% surface expression by chemiluminescence, respectively) showed mostly core-glycosylated band, with very little complex-glycosylated SUR1 protein.

Next, to assess how each substitution affected ATP-induced inhibition of K_{ATP} channel activity, inside-out patch voltage clamp recordings were performed in transiently transfected COSm6 cells. Because of significantly reduced surface expression in most mutants, cells were pretreated with 300 µM tolbutamide overnight, which partially corrects the trafficking defect caused by R74W, as reported previously (Yan et al., 2004, 2007; Pratt et al., 2009), as well as all other R74 mutations, with the exception of R74D (Fig. S1). Because R74D had no detectable surface expression before or after tolbutamide exposure, it was not analyzed. Tolbutamide was washed out for 2 h before recording. Representative traces for several mutants are shown in Fig. 2 A. Macroscopic currents were exposed to ATP (0.01, 0.1, 0.3, 1, and 3 mM), and the amount of current inhibition relative to maximum channel activity in the absence of ATP was fit to a Hill function as described in Materials and methods to

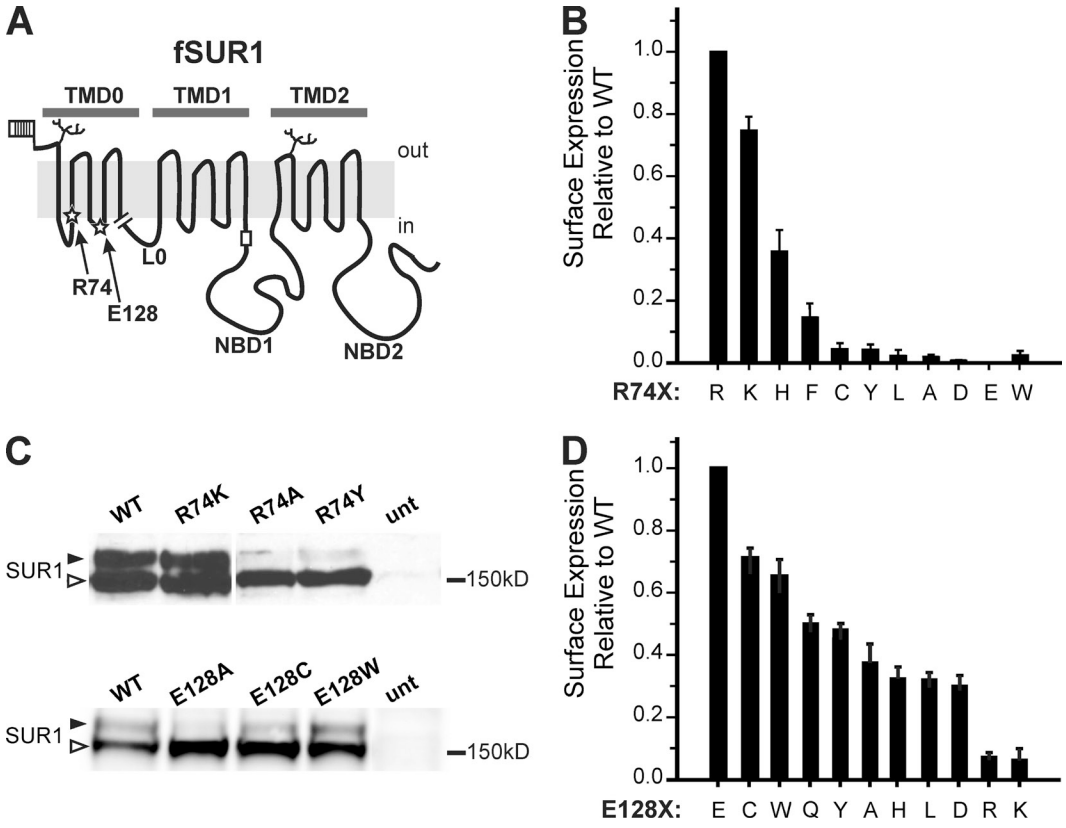

Figure 1. Expression studies of fSUR1 R74X and E128X K_{ATP} channels. (A) Schematic of fSUR1 structure including topological domains and the placement of residues R74 and E128 (stars), glycosylation sites (branches), extracellular FLAG epitope (flag), and the RKR–ER-retention motif (rectangle). The end of the TMD0 (amino acid 198) construct used in subsequent experiments is shown by the break. (B) Chemiluminescence assays were performed to quantitatively assess how surface expression of K_{ATP} channels is affected by different amino acids at position 74 of SUR1. Surface expression is shown relative to WT channel expression. Error bars represent SEM; n = 3–6 for each condition. (C) Representative immunoblots using anti-SUR1 antibody to detect expression of fSUR1 protein in cells cotransfected with Kir6.2 and either fSUR1 R74X (top) or E128X (bottom) cDNAs. SUR1 protein undergoes differential glycosylation, such that core-glycosylated protein (bottom band, open arrow head) becomes complex glycosylated (top band, filled arrow head) upon trafficking through the Golgi; thus, the amount of top band is a proxy for the extent of K_{ATP} channel surface expression. Note the blots shown for R74X and E128X are from two separate experiments; therefore, signal intensity should be compared within each blot only. (D) Chemiluminescence assays performed to assess surface expression of E128X K_{ATP} channels. Surface expression is shown relative to WT channel expression. Error bars represent SEM; n = 3–6 for each condition.

obtain the IC_{50} for ATP inhibition (Fig. 2 B). As with trafficking, the charge-conserving mutant R74K had minimal effect on ATP inhibition (IC_{50} = 18 ± 2 and 17 ± 1 µM for WT and R74K, respectively). Additionally, mutation to glutamate (charge reversal), cysteine, and alanine resulted in negligible differences (IC_{50} = 15 ± 1, 20 ± 1, and 24 ± 3 µM, respectively), indicating that although each mutation decreases steady-state surface expression (Fig. 1 B), functional interactions between SUR1 and Kir6.2 are preserved. In contrast, replacement of R74 with aromatic residues resulted in a significant rightward shift in ATP-induced inhibition (IC_{50} = 60 ± 8, 89 ± 14, and 118 ± 6 µM for phenylalanine, tyrosine, and tryptophan [Pratt et al., 2009], respectively).

R74 mutations in TMD0 constructs reduce steady-state protein levels and disrupt surface expression of mini-K_{ATP} channels

Assessing the specific effects of R74X mutations on TMD0 is possible using a truncated SUR1 construct (amino acids 1–198). Steady-state levels of total cellular fTMD0 harboring R74X were assessed via Western blot. R74K had the highest level, with 70% of WT; all other R74 substitutions (alanine, phenylalanine, tyrosine, and tryptophan) resulted in significantly decreased TMD0 levels, with <25% of WT (Fig. 3, A and B), possibly a result of increased degradation. Next, we examined the surface expression of R74W and R74K fTMD0 when coexpressed with Kir6.2ΔC36 using immunofluorescent

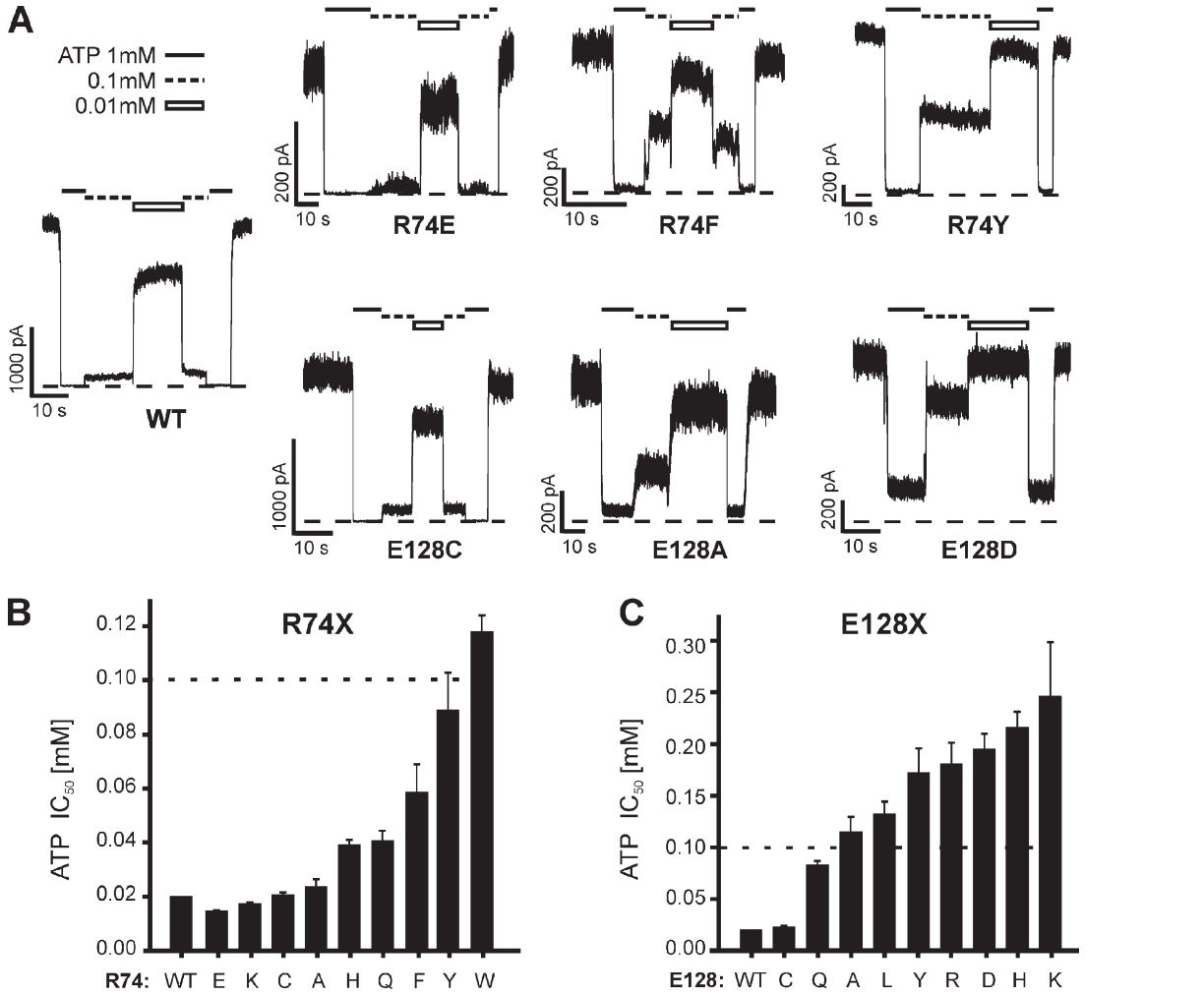

Figure 2. Functional studies of fSUR1 R74X and E128X K_{ATP} channels. (A) Representative traces from inside-out voltage clamp experiments performed in COSm6 cells transfected with WT Kir6.2 and WT, R74X (top), or E128X (bottom) SUR1. ATP concentrations are indicated above each trace (black line, 1 mM; dotted line, 0.1 mM; white bar, 0.01 mM), and zero current is indicated by the dotted line. Bars: horizontal, 10 s; vertical, 1,000 pA for WT and E128C, and 200 pA for the rest. (B and C) ATP sensitivity expressed as half-maximal inhibitory concentration (IC_{50}) for each R74X (B) and E128X (C) mutant. IC_{50} values are from best fits using the Hill equation ($Irel = 1/(1 + ([ATP]/ IC_{50})^H)$). Five ATP concentrations were tested (0.01, 0.1, 0.3, 1, and 3 mM). n = 3–11 patches for each ATP concentration tested. Note that the axes have different ranges for each mutagenesis set: a dotted line denotes the 0.1-mM value on each.

staining. No surface fTMD0 was detected above background signal using anti-FLAG antibody for either mutant construct, even though the R74K mutation exhibited the greatest total TMD0 level (~70% of WT; Fig. 3 B); in contrast, surface staining of cells expressing WT mini-K_{ATP} channels was clearly visible (Fig. 3 E). Consistently, in single-channel recordings from cells coexpressing R74K or R74W fTMD0 with Kir6.2ΔC36, no channel kinetics distinct from those characteristic of channels formed by Kir6.2ΔC36 alone were observed (unpublished data). Collectively, the above observations suggest that mutations at this position likely lead to misfolding and instability of TMD0, thus diminishing physical association with Kir6.2 and preventing the formation of mini-K_{ATP} channels.

Effects of amino acid substitution at E128 of SUR1 on full-length channel biogenesis and ATP sensitivity

As with R74, we performed amino acid substitution studies at position E128 and assessed both surface expression (Fig. 1) and ATP inhibition (Fig. 2) of each mutant. Broadly, E128X mutants showed greater surface expression than R74X mutants. Of the E128X channels tested, charge-reversal mutations (E128R and K) impeded surface expression most strongly (8 and 6% of WT, respectively). Interestingly, the charge-conserving mutation E128D also showed relatively poor surface expression, only 38% that of WT channels. Next, ATP-induced inhibition of E128X-mutant channels was examined. Again, cells were pretreated with 300 µM tolbutamide overnight to increase the surface expression

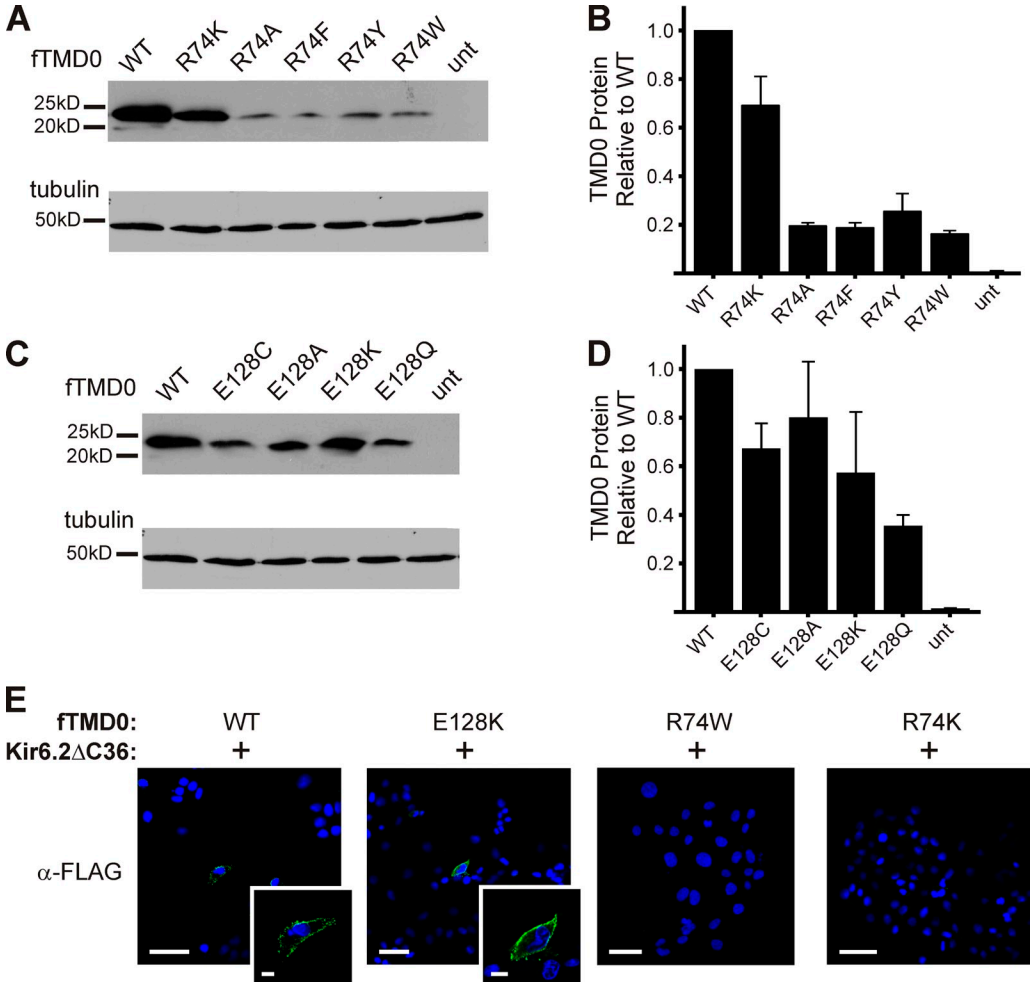

Figure 3. Biochemical and immunostaining studies of TMD0 harboring select R74X or E128X mutations. (A and C) Representative immunoblots of FLAG-tagged SUR1 TMD0 constructs with either R74X (A) or E128X (C) mutations expressed in COSm6 cells. Blots were probed for fTMD0 (α-FLAG) followed by α-tubulin as a loading control. (B and D) Densitometry analysis was performed on the blots in A and C to quantify R74X (B) or E128X (D) fTMD0 protein levels relative to WT fTMD0. $n = 3$. (E) Cells cotransfected with WT, R74W, R74K, or E128K fTMD0 and Kir6.2ΔC36 were probed with α-FLAG antibody 48 h after transfection to detect surface expression of mini-K_{ATP} channels. A rim of surface staining was detected in WT- and E128K-transfected cells (green, inset images), but not in either R74W- or R74K-transfected cells. Cell nuclei were DAPI stained (blue). Bar: 50 mm; insets, 10 mm.

of each E128X mutant (Fig. S1), followed by a 2-h washout before recording. Replacement of E128 with cysteine resulted in WT-like ATP inhibition (IC_{50} = 23 ± 1 μM), but other amino acid substitutions significantly decreased ATP inhibition (Fig. 2, A and C). Of note, the substitution of E128 with tryptophan resulted in a unique inactivation phenotype in which the current undergoes rapid spontaneous decay in the absence of ATP (discussed below; see Fig. 8), making it difficult to assess the extent of ATP-induced current inhibition and the IC_{50} value for this mutation.

E128 mutations disrupt functional coupling between TMD0 and Kir6.2 in mini-K_{ATP} channels

E128X substitutions affect K_{ATP} channel surface expression and ATP sensitivity in a pattern distinct from R74X substitutions. This suggests different roles of the two residues in channel structure and function. To further investigate how E128 contributes to K_{ATP} channel physiology, we analyzed E128X TMD0 proteins and the resulting mini-K_{ATP} channels when coexpressed with Kir6.2ΔC36. Western blots of fTMD0 showed that E128 mutations did not decrease steady-state total cellular TMD0 levels as much as R74 mutations (Fig. 3, C and D). Also in contrast to R74X, E128K fTMD0 was detected at the cell surface of COSm6 cells when cotransfected with Kir6.2ΔC36 (Fig. 3 E), indicating that the formation of mini-K_{ATP} channels is suitable for electrophysiological analysis.

Previously, we reported that full-length K_{ATP} channels with the E128K mutation in SUR1 have decreased intrinsic P_o (P_o = 0.18 vs. 0.63 for WT; Pratt et al., 2009). We tested whether the same would be true for E128K mini-K_{ATP} channels, which would be a clear indication

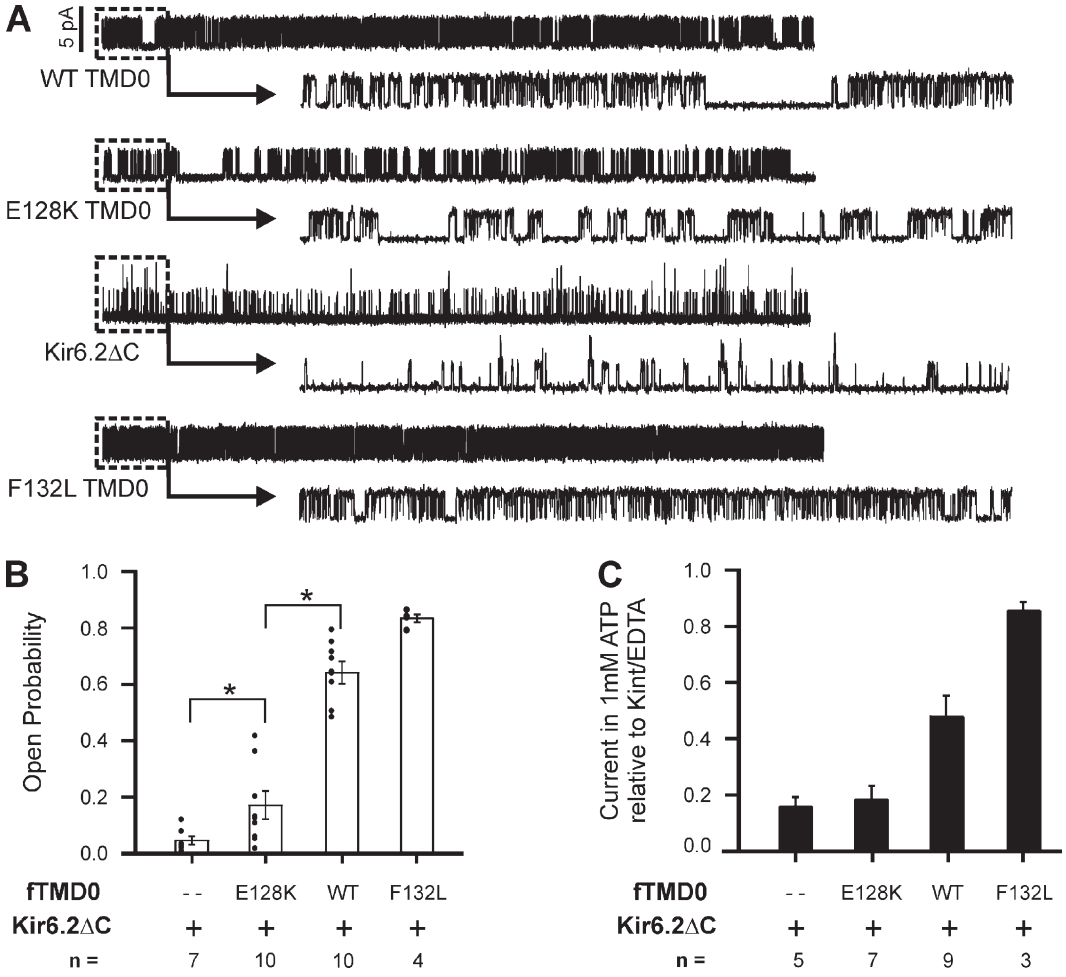

Figure 4. E128K mini-K_{ATP} channels have decreased intrinsic P_o. (A) Representative traces from inside-out voltage clamp recordings made from COSm6 cells transfected with Kir6.2ΔC36 (denoted as Kir6.2ΔC) alone or with WT, E128K, or F132L fTMD0 to form mini-K_{ATP} channels. Each trace is 10-s long (upper), with 1 s expanded (dashed box, lower) to illustrate bursting properties. The scale bar near the WT trace is 5 pA and applies to all traces. (B) Average intrinsic P_o of each channel type is given ±SEM. Distribution of individual data points and the number of patches analyzed are also shown. The average P_o of E128K mini-K_{ATP} channels is significantly different from WT mini-K_{ATP} channels and Kir6.2ΔC36 channels (*, $P < 0.05$; Student's *t* test). (C) Average current of mini-K_{ATP} and Kir6.2ΔC36 channels in 1 mM ATP relative to maximal current in nucleotide-free Kint/EDTA solution. The number of inside-out patches tested is given; error bars represent SEM.

that E128K disrupts functional coupling between TMD0 and Kir6.2. Single-channel recordings made from COSm6 cells cotransfected with E128K fTMD0 and Kir6.2ΔC36 showed that the average intrinsic P_o of E128K mini-K_{ATP} channels was, indeed, significantly lower than WT mini-channels (P_o = 0.17 ± 0.04 for E128K vs. 0.60 ± 0.06 for WT; P < 0.05) (Fig. 4, A and B). Further, the E128K mini-channels exhibited short bursts of activity separated by relatively long closures, distinguishing them from WT mini-channels and channels composed of Kir6.2ΔC36 alone. Mini-K_{ATP} channels with the F132L mutation were used as a positive control; F132L was identified in patients with severe neonatal diabetes and has been shown to increase intrinsic P_o in full-length and mini-K_{ATP} channels (Proks et al., 2006, 2007). These results demonstrate that E128K in both full-length SUR1 and TMD0 alone reduces functional coupling to Kir6.2 with regard to intrinsic P_o and single-channel kinetics.

In K_{ATP} channels, sensitivity to ATP inhibition is normally negatively correlated with intrinsic P_o through allosteric effects (Enkvetchakul et al., 2000; Enkvetchakul and Nichols, 2003). Accordingly, in mini-K_{ATP} channels, TMD0 increases the P_o but decreases the ATP sensitivity of Kir6.2ΔC36 (IC_{50}, ∼138 µM for Kir6.2ΔC36 and ∼309 µM for TMD0 plus Kir6.2ΔC36; Chan et al., 2003). Because E128K abrogated the effect of TMD0 on the P_o of Kir6.2, we predicted that mini-K_{ATP} channels with the E128K mutation will have an ATP sensitivity similar to Kir6.2ΔC36 channels. WT, E128K, or F132L mini-channels or Kir6.2ΔC36 channels expressed in COSm6 cells were studied in the absence and presence of 1 mM ATP (Fig. 4 C). Again, the F132L mini-channels were included as a control because they have increased P_o and decreased ATP sensitivity compared with WT mini-K_{ATP} channels (Proks et al., 2007). As predicted, the E128K mini-channels were inhibited to a similar extent as Kir6.2ΔC36 channels (∼85%), whereas the WT and F132L mini-channels were inhibited by only 52 and 15%, respectively (compare Fig. 4, B and C). This result provides further evidence that E128K directly uncouples functional interactions between TMD0 and Kir6.2, thus preventing the influence TMD0 has on the P_o and ATP sensitivity of Kir6.2ΔC36 channels.

E128K attenuates the response of full-length channels to PIP_2

The intrinsic P_o of Kir channels is thought to be determined by channel interactions with membrane phosphoinositides, in particular, PIP_2: the stronger the interactions, the higher the P_o (Logothetis et al., 2007; Xie et al., 2007). In K_{ATP} channels, PIP_2 increases the P_o and allosterically decreases the apparent sensitivity to ATP inhibition (Baukrowitz et al., 1998; Shyng and Nichols, 1998; Fan and Makielski, 1999). Additionally, previous studies have shown that although Kir6.2 interacts with PIP_2 directly, SUR1 enhances Kir6.2 response to PIP_2 (Baukrowitz et al., 1998; Shyng and Nichols, 1998; Enkvetchakul et al., 2000). In inside-out patches, the application of PIP_2 to the bath solution rapidly increases WT channel

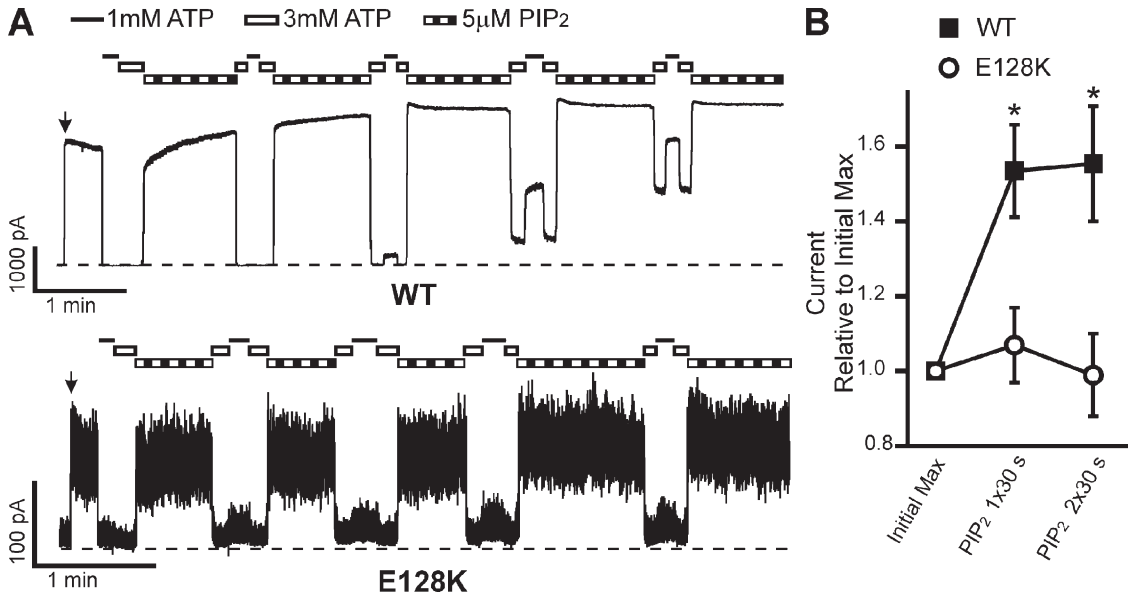

Figure 5. E128K full-length K_{ATP} channels have decreased PIP_2 response. (A) Traces of inside-out voltage clamp recordings from COSm6 cells transfected with Kir6.2 and WT (top) or E128K (bottom) SUR1. Patches were exposed to 1 mM (black line) or 3 mM (white bar) ATP or 5 µM PIP_2 (striped bar). Bars: WT, 1 min and 1,000 pA; E128K, 1 min and 100 pA. Zero current is indicated by the dotted lines. (B) Average change of currents relative to the initial maximum current upon excision into ATP-free Kint/EDTA solution (arrows in A) after one or two sequential 30-s exposures to 5 µM PIP_2. Error bars represent SEM; n = 8 (WT) and 12 (E128K) patches (*, P < 0.05; Student's t test).

activity to maximal P_o and decreases channel sensitivity to ATP inhibition. In contrast, Kir6.2ΔC36 channels show a relatively small increase in P_o and a decrease in ATP sensitivity. We hypothesize that SUR1 modulates the P_o of Kir6.2 via TMD0 by enhancing channel response to PIP_2. Moreover, E128 is essential for this modulation, as shown by the diminished effect E128K TMD0 had on the P_o of Kir6.2 (Fig. 4). Accordingly, we predicted that the E128K channel will have reduced sensitivity to PIP_2. Indeed, we found that K_{ATP} channels harboring the E128K mutation were much less responsive to PIP_2, both in terms of increase in current amplitude (i.e., P_o) and decrease in ATP inhibition compared with WT.

The effect of PIP_2 on the current amplitude of WT and E128K channels was first examined using our standard recording protocol in which membrane patches were excised into Kint bath solution containing 1 mM EDTA, which prevents channel rundown (Lin et al., 2003). After 30 s of exposure to 5 μM PIP_2, WT current increased 1.53 ± 0.12–fold relative to current before PIP_2 exposure, whereas E128K channel current increased only 1.07 ± 0.10–fold (Fig. 5, A and B). An additional 30-s exposure to 5 μM PIP_2 did not minimize this difference. The lack of current increase upon PIP_2 exposure in E128K is striking when one considers that the starting P_o of E128K is so much lower than WT, such that WT P_o has the potential to increase from ∼0.6 to 1.0, whereas E128K P_o has the potential to increase from ∼0.2 to 1.0. To further illustrate the differential response in WT and E128K channels with respect to PIP_2-induced current amplitude increase, we excised membrane patches into Kint plus 1 mM Mg^{2+} to induce rundown, such that WT channel P_o before PIP_2 exposure was substantially reduced (Fig. 6). Under this condition, successive exposures to PIP_2 led to a much more pronounced current increase in WT channels, well beyond the initial current immediately after patch excision (2.1 ± 0.5, 2.3 ± 0.7, and 2.3 ± 0.6 after one, two, and three PIP_2 exposures, respectively; Fig. 6 B). In contrast, successive exposures of E128K channels to PIP_2 after rundown also led to recovery of channel activity, but the current amplitude never reached that seen before rundown, such that the fold change in current amplitude relative to the initial current after successive 30-s PIP_2 exposures was only ∼0.5 for E128K (0.4 ± 0.1, 0.5 ± 0.1, and 0.5 ± 0.1 after one, two, and three PIP_2 exposures, respectively; Fig. 6 B). Interestingly, we noted that the E128K channels were

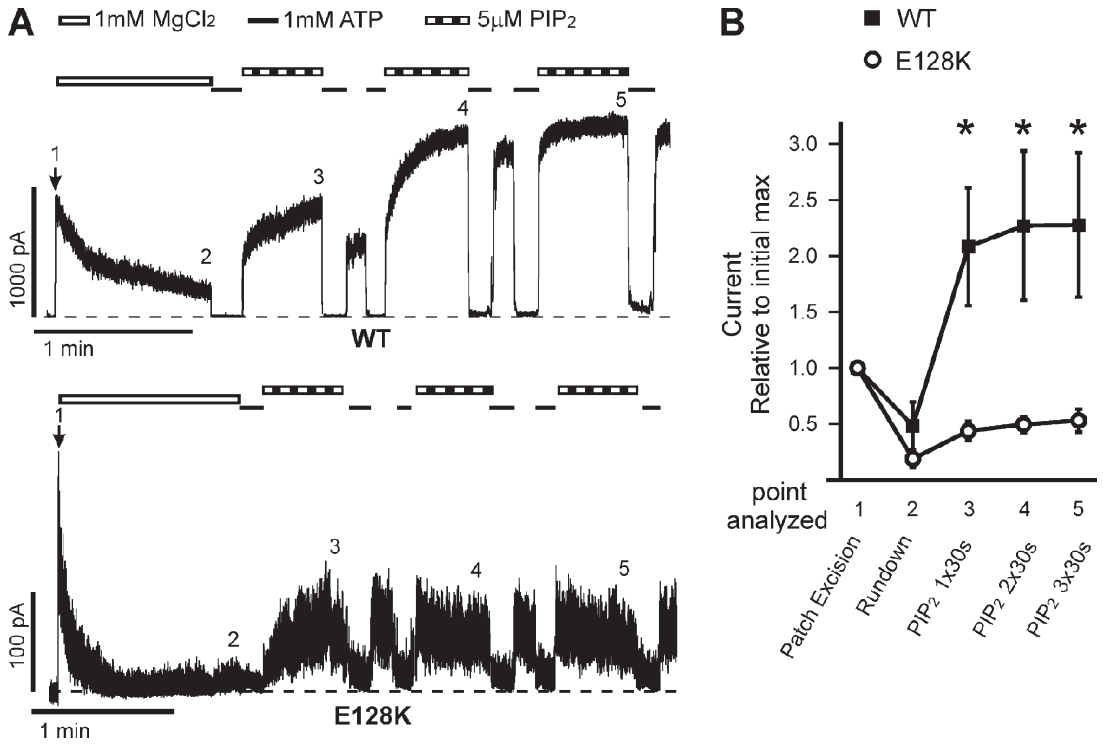

Figure 6. Rundown induced by 1 mM Mg^{2+} enhances the difference between WT and E128K response to PIP_2 stimulation. (A) Representative inside-out patch voltage clamp recordings from COSm6 cells transfected with WT (top) or E128K (bottom) K_{ATP} channels. Patches were pulled into Kint plus 1 mM $MgCl_2$ for 1 min to induce rundown to accentuate the differential response between WT and E128K channels; EDTA was not included in any of the solutions. Patches were then exposed to either 1 mM ATP or 5 μM PIP_2. Bars: WT, 1 min and 1,000 pA; E128K, 1 min and 100 pA. Zero current is indicated by the dotted lines. Time of patch excision is noted by the arrow. (B) Change in current is expressed as the average current at each experimental time point relative to the initial maximum immediately upon patch excision. The change in current was determined after rundown and after one, two, or three 30-s exposures to 5 μM PIP_2; the point of each record analyzed is indicated by the numbers above each trace in A. Error bars represent SEM. n = 5–8 for each data point (*, $P < 0.05$; Student's t test comparing WT and E128K for each point analyzed).

more susceptible to Mg^{2+}-induced rundown, consistent with weakened interactions with PIP_2.

PIP_2 reduces ATP inhibition in WT channels. This effect was also abrogated in the E128K mutant. Patches containing WT or E128K channels were excised into Kint/EDTA solution and then exposed to differing concentrations of ATP (Fig. 7 A). In WT channels, successive exposures to 5 μM PIP_2 led to a significant decrease in the amount of current inhibited by ATP, causing a significant rightward shift in ATP dose–response (the change in ATP dose–response after three PIP_2 treatments is shown in Fig. 7 B). However, in E128K channels, exposure to PIP_2 had little effect on ATP inhibition (Fig. 7, A and C). Collectively, the reduced response to PIP_2 in the E128K channels resembles that seen in Kir6.2ΔC36 channels, providing evidence that E128K disrupts the ability of SUR1 to enhance channel response to PIP_2.

The E128W mutation in SUR1 causes inactivation in full-length channels that can be recovered by PIP_2 and by exposure and subsequent removal of ATP

Additional evidence supporting the involvement of E128 in mediating channel response to PIP_2 came from the intriguing phenotype observed with the E128W mutation. As mentioned above, the mutation of E128 to a tryptophan causes the current to undergo spontaneous decay in the absence of nucleotides, which we refer to as inactivation (Fig. 8). This inactivation is distinct from rundown in WT channels in that inactivation occurs despite the presence of 1 mM EDTA, which we have shown previously to be highly effective in preventing rundown in WT channels (Lin et al., 2003). Inactivation of E128W channels could be recovered by exposure to high concentrations of ATP (1, 3, or 5 mM) in a time-dependent manner, such that lengthening the time of ATP exposure resulted in more current when the patch was reexposed to nucleotide-free solution (Fig. 8, A and B). Further, exposure of the E128W patches to PIP_2 slowed or reversed the inactivation as well as potentiated the ATP-induced "resetting" of channel activity (Fig. 8 C). These results indicate that E128W causes K_{ATP} channel inactivation by destabilizing PIP_2–K_{ATP} channel interactions, and that ATP exposure reestablishes the interactions as seen in the transient channel activity when the inhibitory effect of ATP is removed.

DISCUSSION

Biochemical, functional, and structural studies to date have provided clear evidence that TMD0 of SUR1 interacts with Kir6.2 to modulate channel trafficking and

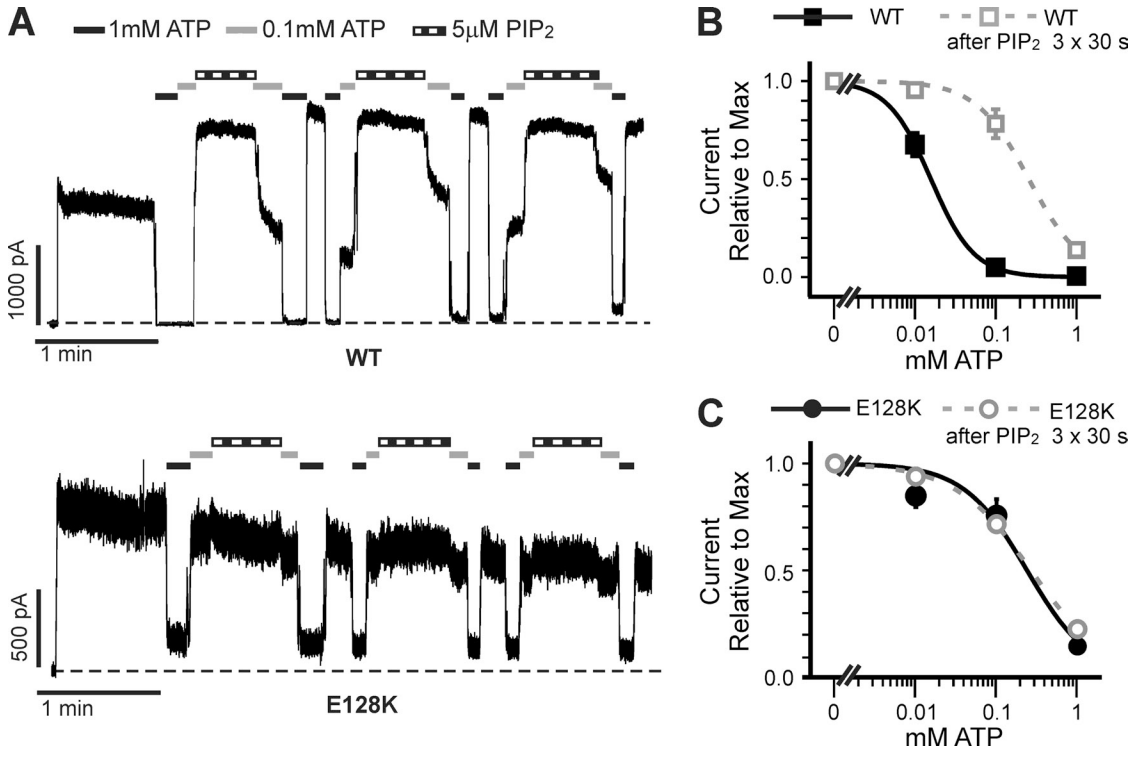

Figure 7. Decrease of ATP sensitivity in response to PIP_2 is abrogated by the E128K mutation. (A) Representative inside-out patch voltage clamp recordings from COSm6 cells transfected with WT (top) or E128K (bottom) K_{ATP} channels. Bars: WT, 1 min and 1,000 pA; E128K, 1 min and 500 pA. Zero current is indicated by the dotted lines. (B and C) Current inhibition by ATP was assessed using several ATP concentrations (0.01, 0.1, and 1 mM) before PIP_2 exposure (filled black symbols) and after three 30-s exposures to 5 μM ATP (open gray symbols) for WT (B) and E128K (C) channels. A best fit for each dose–response was calculated using the Hill equation (before PIP_2 exposure: solid lines; after PIP_2 exposure: dotted lines). Error bars represent SEM. $n = 4$–8 patches for each data point.

gating (Schwappach et al., 2000; Babenko and Bryan, 2003; Chan et al., 2003; Mikhailov et al., 2005). However, the signaling mechanism(s) by which TMD0 exerts its effects remains poorly understood. Mutations in TMD0 such as R74W and E128K offer potential for probing the molecular basis of TMD0-Kir6.2 signaling, as they cause dramatic impediments to channel trafficking and gating. Here, we studied full-length and mini-K_{ATP} channels to learn more about the functional roles of R74 and E128. We show that R74W and E128K disrupt channel function by different mechanisms. Importantly, our results reveal that TMD0 controls gating of the Kir6.2 pore by modulating PIP_2 sensitivity.

Role of R74

The replacement of R74 by any nonconserved residue in full-length channels led to a substantial decrease in surface expression (Fig. 1 B). That these mutations also cause a dramatic reduction in TMD0 protein levels (Fig. 3, A and B) suggests an important role of R74 in structural integrity of this protein domain. Although the exact location of R74 with respect to the membrane has not been determined experimentally, in silico calculations (using the TOPCONS algorithm; Bernsel et al., 2009) predict that R74 resides at the cytosolic end of the second transmembrane (TM) segment of TMD0 (Fig. S2). Studies of membrane integration of proteins have shown that the aromatic amino acids tryptophan and tyrosine are frequently found at the membrane–water interface where they interact favorably with the lipid head groups, whereas another aromatic residue, phenylalanine, favors placement deeper into the lipophilic environment of the membrane (Killian and von Heijne, 2000). Charged amino acids are more likely to be found in cytoplasmic aqueous environments (Heijne, 1986). However, positively charged amino acids lysine and arginine, which have relatively long aliphatic side chains, are also seen at the interface where the aliphatic chain is localized to the hydrophobic part of the lipid bilayer, whereas the charged side chains interact with negatively charged lipid phosphate groups (Killian and von Heijne, 2000; Hessa et al., 2005). The relevance of these patterns of TM segment properties to the results presented

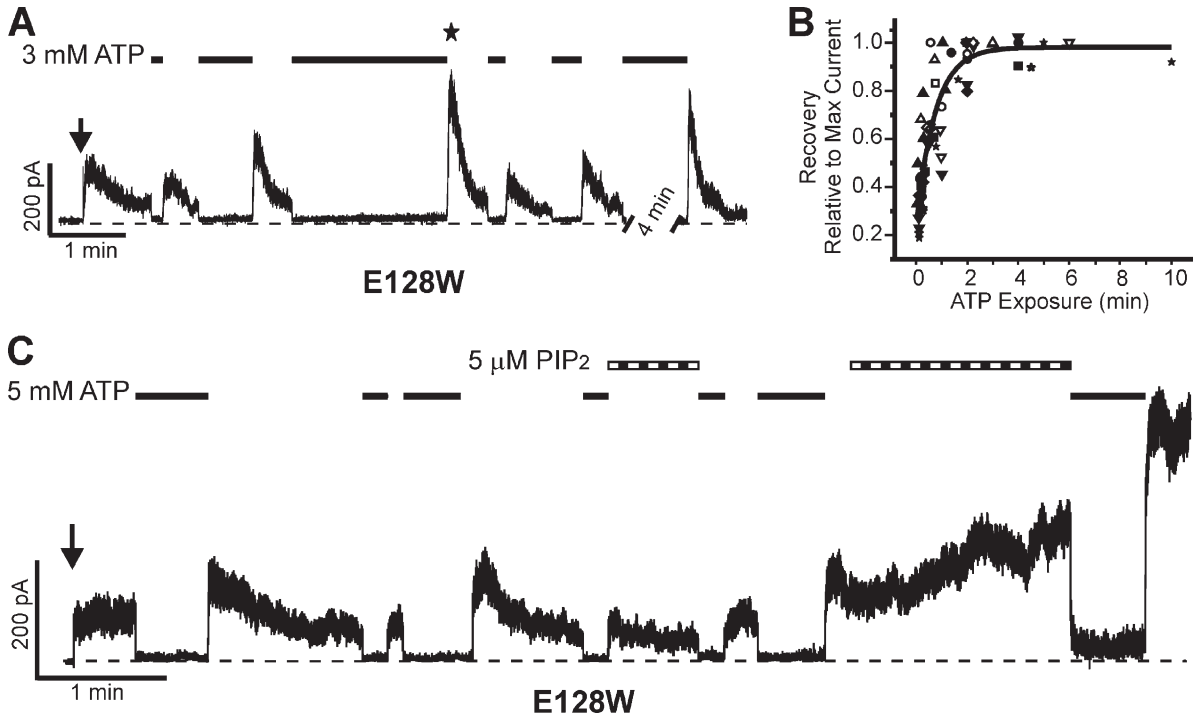

Figure 8. E128W causes K_{ATP} channel inactivation that can be recovered by ATP exposure and subsequent removal of ATP and can be reversed by PIP_2. (A) Representative trace of inside-out voltage clamp experiment showing inactivation and the ability of ATP to "reset" the current upon reentry into ATP-free Kint/EDTA solution. The time of patch excision is denoted by the arrow, 3-mM ATP exposure by the black lines, and the zero current level by the dotted line. The maximal current for this record is indicated by the star. Bars: vertical, 200 pA; horizontal, 1 min. Note the break in trace during which ATP was applied. (B) The ability of high concentrations (1–5 mM) of ATP to reset the E128W K_{ATP} channel is illustrated by this scatter plot. Each symbol represents a different trace with several exchanges between ATP-containing and ATP-free Kint/EDTA solutions (the values for the trace in A are solid squares). 12 traces are represented. The amount of current upon reexposure to Kint/EDTA (y axis) is dependent on the length of time the patch is exposed to ATP (x axis). The collective dataset is well represented by an exponential fit. (C) Representative trace showing that exposure of the E128W K_{ATP} channels to 5 μM PIP_2 (striped bars) decreased and reversed inactivation as well as increased the efficacy of ATP (black lines, 5 mM) to reset the channel. PIP_2 also decreased the ability of ATP to inhibit channel activity, as seen after the second PIP_2 exposure. Bars: 1 min and 200 pA.

here comes into play when hypothesizing the structural changes R74X substitutions have on TMD0 conformation. One might expect that the substitution of TM-flanking R74 by nonconserved amino acids will induce a shift of the TM2 boundary and/or disrupt normal membrane integration. Accordingly, with the exception of lysine, all other amino acids used in the R74X screen (A, H, C, W, F, Y, L, D, or E) are predicted to shift the boundary of TM1 and TM2 (as well as TM3 for R74D and R74E) by TOPCONS (Fig. S2). The decrease in full-length K_{ATP} channel surface expression of R74X mutants (Fig. 1) and steady-state protein levels of TMD0 (Fig. 3) is consistent with these substitutions having an effect on protein structure and stability.

Sulfonylureas acting as chemical chaperones partially overcome the trafficking defect in R74X full-length K_{ATP} channels, with the exception of R74D (Fig. S1). Although the mechanism by which sulfonylureas overcome this defect is not yet known, this rescue strategy provides us the opportunity to analyze the ATP sensitivity of most mutants. Our results show that the mutation of R74 reduces ATP inhibition of the channel. Unfortunately, however, R74X TMD0 mutants failed to express at the cell surface when coexpressed with Kir6.2ΔC36, making it difficult to address the question of whether the gating defects in full-length channels are caused by changes in the functional coupling between TMD0 and Kir6.2 or are a consequence of altered influences by SUR1 structures outside TMD0. It may seem surprising that although total R74K TMD0 protein remains at near WT levels (Fig. 3, A and B), no R74K mini-channels were observed at the cell surface either by immunostaining or single-channel recording. That the R74K mutation has a more pronounced effect on the surface expression of mini-K_{ATP} versus full-length channels (i.e., no detectable surface expression of mini-channels [Fig. 3 C] vs. 80% of WT for full-length channels [Fig. 1, B and C]) suggests a role for extra-TMD0 regions of SUR1 in channel protein folding and assembly. In the water channel aquaporin-1, membrane integration of N-terminal TM segments requires the translation of subsequent TM segments (Skach et al., 1994), and protein stability is correlated to membrane integration of the channel subunits (Buck and Skach, 2005). Thus, the

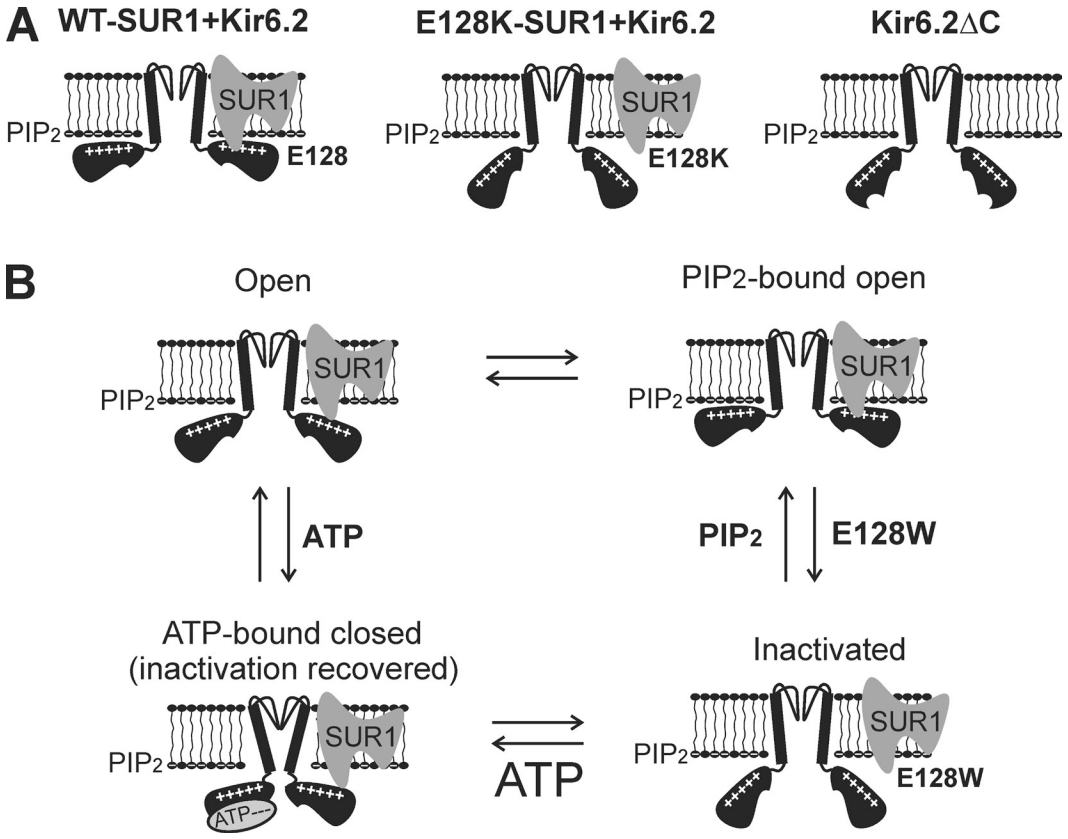

Figure 9. Proposed model for the role of E128 in SUR1-Kir6.2 coupling. (A) Cartoon illustrating proposed physical relationships between SUR1, Kir6.2, and PIP_2 in the WT, E128K mutant, and the Kir6.2ΔC36 channels. (B) The E128W mutation destabilizes the channel in the SUR1-Kir6.2–coupled, PIP_2-bound open state, leading to channel inactivation. These structural changes can be overcome by increasing membrane PIP_2 or by ATP binding to the channel that recovers coupling between SUR1 and Kir6.2, allowing channels to enter the PIP_2-bound open state briefly before inactivation occurs again. Note that the four states presented should not be taken as detailed kinetic gating states of the channel, and that the transitions between the states are indicated only to illustrate the recovery effects of PIP_2 and ATP on inactivated channels.

tertiary structure of R74K TMD0 and its ability to assemble with Kir6.2 to form channels may be contingent upon the SUR1 structures downstream of TMD0.

Role of E128

Full-length channels bearing E128X mutations are in general expressed at a higher level at the cell surface than R74X channels (Fig. 1). Moreover, mutations at residue 128 have less effect on TMD0 protein levels, and E128K TMD0 can form mini-channels with Kir6.2ΔC36 that traffic to the cell surface (Fig. 3). These results suggest that E128 is not as critical for the folding of TMD0 as R74. Consistent with this idea, the TOPCONS-predicted TM structure of TMD0 does not change with any E128 substitution, in contrast to substitutions at R74 (Fig. S2). However, the E128K mutation in both full-length and mini-K_{ATP} channels shifts the P_o and ATP sensitivity toward those seen in Kir6.2ΔC36 channels, indicating that E128 contributes to functional coupling with Kir6.2.

Strikingly, E128K renders full-length channels much less sensitive to PIP_2 stimulation, resembling that seen in Kir6.2ΔC36 channels. To our knowledge, this is the first SUR1 mutation reported to reduce channel sensitivity to PIP_2. The finding is important because although SUR1 has been implicated in K_{ATP} channel gating regulation by PIP_2, the mechanisms are unknown (Baukrowitz et al., 1998; Enkvetchakul et al., 2000; Song and Ashcroft, 2001). The current model is that the charged phosphoinositol head group of PIP_2 binds to Kir6.2 via a patch of positively charged residues in the cytoplasmic domain near the plasma membrane (Nishida and MacKinnon, 2002; Enkvetchakul and Nichols, 2003; Kuo et al., 2003). This portion of Kir6.2 is "pulled" toward the membrane, resulting in a stabilized open conformation. Our study identifies a residue in SUR1 that is critical to this regulation. How might E128 contribute to channel interaction with PIP_2? Because E128 is negatively charged, it probably does not participate directly in PIP_2 (or ATP) binding. Instead, we propose that E128 interacts directly with Kir6.2 near the membrane–cytoplasm interface to stabilize the channel in a PIP_2-bound open state (Fig. 9 A). This is consistent with the predicted location of E128 within the short second cytoplasmic loop adjacent to the lipid bilayer. The idea that TMD0 increases the P_o of Kir6.2 by enhancing channel–PIP_2 interactions differs from a previous model in which intramembrane interactions between TMD0 and Kir6.2 reposition the Kir6.2 outer helix to achieve the gating effect (Babenko and Bryan, 2003).

It is well accepted that PIP_2 is a primary determinant of channel P_o. The detrimental effect of E128K on channel interaction with PIP_2 therefore offers a clear explanation for how the mutation reduces P_o in full-length and mini-K_{ATP} channels. However, the explanation for the effects of E128K on ATP sensitivity in full-length and mini-K_{ATP} channels is more complex. Previous studies have shown that although TMD0 confers high intrinsic P_o to Kir6.2 in full-length channels, it does not confer the high ATP sensitivity mediated by SUR1 (Babenko and Bryan, 2003; Chan et al., 2003). Accordingly, mini-K_{ATP} channels composed of TMD0 and Kir6.2ΔC36 are even less sensitive to ATP inhibition than Kir6.2ΔC36 channels, following the model that increased P_o (as a result of enhanced PIP_2 interactions) allosterically reduces ATP inhibition. Mini-K_{ATP} channels with the E128K mutation also follow this relationship; i.e., they show reduced P_o and increased ATP inhibition relative to WT mini-channels (similar to that seen for Kir6.2ΔC36). Although the inverse relationship between P_o and ATP sensitivity might predict that in full-length channels the E128K mutant should show increased ATP sensitivity relative to WT, this is not the case. Rather, E128K full-length channels actually have reduced ATP inhibition. Thus, by abolishing the ability of TMD0 to enhance Kir6.2 response to PIP_2, the E128K mutation abrogates the ability of structures downstream of TMD0 to confer increased ATP sensitivity to Kir6.2. Future identification of SUR1 residues responsible for increasing ATP sensitivity of the channel will be critical for understanding precisely how E128K uncouples SUR1 from Kir6.2 with respect to regulation by both PIP_2 and ATP.

A novel K_{ATP} channel inactivation mechanism revealed by the E128W mutation and structural implications

The importance of E128 in the structural and functional integrity of K_{ATP} channels is further accentuated by the inactivation phenotype of the E128W mutant. This inactivation phenotype is reminiscent of what we have described previously for several Kir6.2 mutations predicted to disrupt inter-Kir6.2 subunit interactions (Shyng et al., 2000; Lin et al., 2003, 2008). First, current inactivation induced by E128W is distinct from rundown. Second, inactivation caused by E128W is prevented or reversed by PIP_2. Third, inactivation can be recovered by ATP exposure in a time- and concentration-dependent way. We have previously proposed that in the Kir6.2 inactivation mutants, disruption of inter-Kir6.2 subunit interactions destabilizes channels in the PIP_2-bound open state, and that the application of exogenous PIP_2 shifts the equilibrium of channels toward the PIP_2-bound open state to prevent and reverse inactivation (Lin et al., 2003). ATP, which has been proposed to bind to a site coordinated by specific N- and C-terminal residues from adjacent Kir6.2 subunits, reestablishes the subunit–subunit interface, allowing channels to bind PIP_2 and, when the ATP inhibitory effect is removed, to open briefly (Lin et al., 2003). That inactivation induced by E128W is overcome by PIP_2 lends strong support to our proposal that E128 plays a critical role in the stabilization of Kir6.2–PIP_2 interactions by SUR1. In addition, the ATP-dependent recovery from inactivation in the E128W mutant suggests that conformational changes in Kir6.2

brought about by the binding of ATP reestablish functional coupling between SUR1 and Kir6.2, manifested as increased channel activity (i.e., P_o) when ATP inhibition is removed. These findings uncover a novel channel inactivation mechanism involving aberrant SUR1–Kir6.2 interactions and establish a role for E128 in the structural integrity of K_{ATP} channels.

The similar gating properties seen in E128W and Kir6.2 inactivation mutations predicted to alter inter-Kir6.2 subunit interfaces imply that these mutations disrupt normal channel gating via a converging mechanism that is sensitive to both PIP_2 and ATP. Channel structures obtained by crystallography describe an unappreciated role for the intracellular domain (including the membrane-tethered slide helix) in modulating the ion conduction pore of Kir channels (Clarke et al., 2010). Namely, a "twist" conformation in which the slide helix and cytoplasmic domain rotate relative to the TM and pore helices is associated with a nonconducting pattern of ions within the selectivity filter. The transmission of intracellular conformational change into channel opening (involving rearrangement of cytoplasmic subunit–subunit interfaces) occurs in the absence of appreciable changes in TM segment amino acid backbones. This study highlights the importance of intracellular subunit–subunit interactions in Kir channel gating and helps explain how mutations of Kir6.2 residues predicted to lie at the inter-Kir6.2 subunit interface (such as E229, R314, and R301) cause inactivation. The finding is especially provocative when considered in the context of the SUR1–Kir6.2 K_{ATP} channel complex because it opens up the possibility that SUR1 can modulate Kir6.2 conduction primarily through cytoplasmic domain interfaces, such as that mediated by E128. We propose that in K_{ATP} channels, SUR1 stabilizes a Kir6.2 structure in the PIP_2-bound open state via cytoplasmic interactions, and that the inactivation phenotype of E128W represents transition from a SUR1-coupled conformation to Kir6.2 structures lacking the stabilizing effect of SUR1, as seen in Kir6.2ΔC36. ATP binding is envisioned to cause a conformational switch in Kir6.2, such that channels can enter a PIP_2-bound open state once ATP is removed. Thus, in the case of Kir6.2 inactivation mutations, ATP reactivates the channel by reestablishing Kir6.2 subunit interface (Lin et al., 2003), and in the case of E128W, by reestablishing SUR1–Kir6.2 interactions necessary for stabilizing channel opening, albeit only briefly (see Fig. 9 B). Increasing the concentration of PIP_2 in the membrane is expected to shift the equilibrium toward the PIP_2-bound open state by mass action, thereby slowing and reversing inactivation as well as boosting the ATP-induced resetting of the channel in both Kir6.2 and E128W-SUR1 inactivation mutants (Figs. 8 C and 9 B).

In summary, our study shows that R74 and E128 have different roles in TMD0 structure–function. Whereas R74 is important for TMD0 structure stability, E128 is critical for functional coupling between TMD0 and Kir6.2 by controlling channel response to PIP_2. The finding that TMD0 controls Kir6.2 gating via PIP_2 reinforces the concept that in Kir channels, diverse modulators affect channel gating by modulating channel interactions with membrane phospholipids (Logothetis et al., 2007; Xie et al., 2007). Finally, our discovery of the E128W inactivation mutation provides novel insight into the structural relationship between channel subunits as a function of ATP and PIP_2.

We thank Jeremy Bushman and Dr. Qing Zhou for helpful discussions and Joel Gay, Dr. Pei-Chun Chen, and Dr. Yoshihiro Matsumura for technical assistance.

This work was supported by grants from National Institute of Diabetes and Digestive and Kidney Diseases to E.B. Pratt (F30DK081305) and to S.-L. Shyng (DK066485).

Lawrence G. Palmer served as editor.

Submitted: 13 October 2010
Accepted: 21 January 2011

REFERENCES

Aguilar-Bryan, L., and J. Bryan. 1999. Molecular biology of adenosine triphosphate-sensitive potassium channels. *Endocr. Rev.* 20:101–135. doi:10.1210/er.20.2.101

Aguilar-Bryan, L., C.G. Nichols, S.W. Wechsler, J.P. Clement IV, A.E. Boyd III, G. González, H. Herrera-Sosa, K. Nguy, J. Bryan, and D.A. Nelson. 1995. Cloning of the beta cell high-affinity sulfonylurea receptor: a regulator of insulin secretion. *Science.* 268:423–426. doi:10.1126/science.7716547

Antcliff, J.F., S. Haider, P. Proks, M.S. Sansom, and F.M. Ashcroft. 2005. Functional analysis of a structural model of the ATP-binding site of the KATP channel Kir6.2 subunit. *EMBO J.* 24:229–239. doi:10.1038/sj.emboj.7600487

Ashcroft, F.M. 2005. ATP-sensitive potassium channelopathies: focus on insulin secretion. *J. Clin. Invest.* 115:2047–2058. doi:10.1172/JCI25495

Babenko, A.P., and J. Bryan. 2003. Sur domains that associate with and gate K_{ATP} pores define a novel gatekeeper. *J. Biol. Chem.* 278:41577–41580. doi:10.1074/jbc.C300363200

Babenko, A.P., G. Gonzalez, L. Aguilar-Bryan, and J. Bryan. 1999. Sulfonylurea receptors set the maximal open probability, ATP sensitivity and plasma membrane density of K_{ATP} channels. *FEBS Lett.* 445:131–136. doi:10.1016/S0014-5793(99)00102-7

Baukrowitz, T., U. Schulte, D. Oliver, S. Herlitze, T. Krauter, S.J. Tucker, J.P. Ruppersberg, and B. Fakler. 1998. PIP_2 and PIP as determinants for ATP inhibition of K_{ATP} channels. *Science.* 282:1141–1144. doi:10.1126/science.282.5391.1141

Bernsel, A., H. Viklund, A. Hennerdal, and A. Elofsson. 2009. TOPCONS: consensus prediction of membrane protein topology. *Nucleic Acids Res.* 37:W465–468. doi:10.1093/nar/gkp363

Buck, T.M., and W.R. Skach. 2005. Differential stability of biogenesis intermediates reveals a common pathway for aquaporin-1 topological maturation. *J. Biol. Chem.* 280:261–269.

Cartier, E.A., L.R. Conti, C.A. Vandenberg, and S.-L. Shyng. 2001. Defective trafficking and function of KATP channels caused by a sulfonylurea receptor 1 mutation associated with persistent hyperinsulinemic hypoglycemia of infancy. *Proc. Natl. Acad. Sci. USA.* 98:2882–2887. doi:10.1073/pnas.051499698

Chan, K.W., H. Zhang, and D.E. Logothetis. 2003. N-terminal transmembrane domain of the SUR controls trafficking and gating of Kir6 channel subunits. *EMBO J.* 22:3833–3843. doi:10.1093/emboj/cdg376

Chothia, C. 1976. The nature of the accessible and buried surfaces in proteins. *J. Mol. Biol.* 105:1–12. doi:10.1016/0022-2836(76)90191-1

Clarke, O.B., A.T. Caputo, A.P. Hill, J.I. Vandenberg, B.J. Smith, and J.M. Gulbis. 2010. Domain reorientation and rotation of an intracellular assembly regulate conduction in Kir potassium channels. *Cell.* 141:1018–1029. doi:10.1016/j.cell.2010.05.003

Clement, J.P. IV, K. Kunjilwar, G. Gonzalez, M. Schwanstecher, U. Panten, L. Aguilar-Bryan, and J. Bryan. 1997. Association and stoichiometry of K(ATP) channel subunits. *Neuron.* 18:827–838. doi:10.1016/S0896-6273(00)80321-9

Conti, L.R., C.M. Radeke, S.-L. Shyng, and C.A. Vandenberg. 2001. Transmembrane topology of the sulfonylurea receptor SUR1. *J. Biol. Chem.* 276:41270–41278. doi:10.1074/jbc.M106555200

Cukras, C.A., I. Jeliazkova, and C.G. Nichols. 2002a. Structural and functional determinants of conserved lipid interaction domains of inward rectifying Kir6.2 channels. *J. Gen. Physiol.* 119:581–591. doi:10.1085/jgp.20028562

Cukras, C.A., I. Jeliazkova, and C.G. Nichols. 2002b. The role of NH_2-terminal positive charges in the activity of inward rectifier KATP channels. *J. Gen. Physiol.* 120:437–446. doi:10.1085/jgp.20028621

Du, X., H. Zhang, C. Lopes, T. Mirshahi, T. Rohacs, and D.E. Logothetis. 2004. Characteristic interactions with phosphatidylinositol 4,5-bisphosphate determine regulation of kir channels by diverse modulators. *J. Biol. Chem.* 279:37271–37281. doi:10.1074/jbc.M403413200

Enkvetchakul, D., and C.G. Nichols. 2003. Gating mechanism of K_{ATP} channels: function fits form. *J. Gen. Physiol.* 122:471–480. doi:10.1085/jgp.200308878

Enkvetchakul, D., G. Loussouarn, E. Makhina, S.-L. Shyng, and C.G. Nichols. 2000. The kinetic and physical basis of K(ATP) channel gating: toward a unified molecular understanding. *Biophys. J.* 78:2334–2348. doi:10.1016/S0006-3495(00)76779-8

Fan, Z., and J.C. Makielski. 1999. Phosphoinositides decrease ATP sensitivity of the cardiac ATP-sensitive K^+ channel. A molecular probe for the mechanism of ATP-sensitive inhibition. *J. Gen. Physiol.* 114:251–269. doi:10.1085/jgp.114.2.251

Gribble, F.M., S.J. Tucker, and F.M. Ashcroft. 1997. The essential role of the Walker A motifs of SUR1 in K-ATP channel activation by Mg-ADP and diazoxide. *EMBO J.* 16:1145–1152. doi:10.1093/emboj/16.6.1145

Haider, S.A., A.I. Tarasov, T.J. Craig, M.S. Sansom, and F.M. Ashcroft. 2007. Identification of the PIP2-binding site on Kir6.2 by molecular modelling and functional analysis. *EMBO J.* 26:3749–3759. doi:10.1038/sj.emboj.7601809

Heijne, G. 1986. The distribution of positively charged residues in bacterial inner membrane proteins correlates with the trans-membrane topology. *EMBO J.* 5:3021–3027.

Hessa, T., H. Kim, K. Bihlmaier, C. Lundin, J. Boekel, H. Andersson, I. Nilsson, S.H. White, and G. von Heijne. 2005. Recognition of transmembrane helices by the endoplasmic reticulum translocon. *Nature.* 433:377–381. doi:10.1038/nature03216

Hilgemann, D.W., S. Feng, and C. Nasuhoglu. 2001. The complex and intriguing lives of PIP_2 with ion channels and transporters. *Sci. STKE.* 2001:re19. doi:10.1126/stke.2001.111.re19

Inagaki, N., T. Gonoi, J.P. Clement IV, N. Namba, J. Inazawa, G. Gonzalez, L. Aguilar-Bryan, S. Seino, and J. Bryan. 1995. Reconstitution of IKATP: an inward rectifier subunit plus the sulfonylurea receptor. *Science.* 270:1166–1170. doi:10.1126/science.270.5239.1166

Inagaki, N., T. Gonoi, and S. Seino. 1997. Subunit stoichiometry of the pancreatic beta-cell ATP-sensitive K^+ channel. *FEBS Lett.* 409:232–236. doi:10.1016/S0014-5793(97)00488-2

Killian, J.A., and G. von Heijne. 2000. How proteins adapt to a membrane-water interface. *Trends Biochem. Sci.* 25:429–434. doi:10.1016/S0968-0004(00)01626-1

Kuo, A., J.M. Gulbis, J.F. Antcliff, T. Rahman, E.D. Lowe, J. Zimmer, J. Cuthbertson, F.M. Ashcroft, T. Ezaki, and D.A. Doyle. 2003. Crystal structure of the potassium channel KirBac1.1 in the closed state. *Science.* 300:1922–1926. doi:10.1126/science.1085028

Kyte, J., and R.F. Doolittle. 1982. A simple method for displaying the hydropathic character of a protein. *J. Mol. Biol.* 157:105–132. doi:10.1016/0022-2836(82)90515-0

Lin, Y.W., T. Jia, A.M. Weinsoft, and S.-L. Shyng. 2003. Stabilization of the activity of ATP-sensitive potassium channels by ion pairs formed between adjacent Kir6.2 subunits. *J. Gen. Physiol.* 122:225–237. doi:10.1085/jgp.200308822

Lin, Y.W., J.D. Bushman, F.F. Yan, S. Haidar, C. MacMullen, A. Ganguly, C.A. Stanley, and S.-L. Shyng. 2008. Destabilization of ATP-sensitive potassium channel activity by novel KCNJ11 mutations identified in congenital hyperinsulinism. *J. Biol. Chem.* 283:9146–9156. doi:10.1074/jbc.M708798200

Liou, H.H., S.S. Zhou, and C.L. Huang. 1999. Regulation of ROMK1 channel by protein kinase A via a phosphatidylinositol 4,5-bisphosphate-dependent mechanism. *Proc. Natl. Acad. Sci. USA.* 96:5820–5825. doi:10.1073/pnas.96.10.5820

Logothetis, D.E., T. Jin, D. Lupyan, and A. Rosenhouse-Dantsker. 2007. Phosphoinositide-mediated gating of inwardly rectifying K(+) channels. *Pflugers Arch.* 455:83–95. doi:10.1007/s00424-007-0276-5

Margeta-Mitrovic, M., Y.N. Jan, and L.Y. Jan. 2000. A trafficking checkpoint controls GABA(B) receptor heterodimerization. *Neuron.* 27:97–106. doi:10.1016/S0896-6273(00)00012-X

Mikhailov, M.V., J.D. Campbell, H. de Wet, K. Shimomura, B. Zadek, R.F. Collins, M.S. Sansom, R.C. Ford, and F.M. Ashcroft. 2005. 3-D structural and functional characterization of the purified K_{ATP} channel complex Kir6.2-SUR1. *EMBO J.* 24:4166–4175. doi:10.1038/sj.emboj.7600877

Nichols, C.G. 2006. K_{ATP} channels as molecular sensors of cellular metabolism. *Nature.* 440:470–476. doi:10.1038/nature04711

Nichols, C.G., S.-L. Shyng, A. Nestorowicz, B. Glaser, J.P. Clement IV, G. Gonzalez, L. Aguilar-Bryan, M.A. Permutt, and J. Bryan. 1996. Adenosine diphosphate as an intracellular regulator of insulin secretion. *Science.* 272:1785–1787. doi:10.1126/science.272.5269.1785

Nishida, M., and R. MacKinnon. 2002. Structural basis of inward rectification: cytoplasmic pore of the G protein-gated inward rectifier GIRK1 at 1.8 A resolution. *Cell.* 111:957–965. doi:10.1016/S0092-8674(02)01227-8

Pratt, E.B., F.F. Yan, J.W. Gay, C.A. Stanley, and S.-L. Shyng. 2009. Sulfonylurea receptor 1 mutations that cause opposite insulin secretion defects with chemical chaperone exposure. *J. Biol. Chem.* 284:7951–7959. doi:10.1074/jbc.M807012200

Proks, P., A.L. Arnold, J. Bruining, C. Girard, S.E. Flanagan, B. Larkin, K. Colclough, A.T. Hattersley, F.M. Ashcroft, and S. Ellard. 2006. A heterozygous activating mutation in the sulphonylurea receptor SUR1 (ABCC8) causes neonatal diabetes. *Hum. Mol. Genet.* 15:1793–1800. doi:10.1093/hmg/ddl101

Proks, P., K. Shimomura, T.J. Craig, C.A. Girard, and F.M. Ashcroft. 2007. Mechanism of action of a sulphonylurea receptor SUR1 mutation (F132L) that causes DEND syndrome. *Hum. Mol. Genet.* 16:2011–2019. doi:10.1093/hmg/ddm149

Raab-Graham, K.F., L.J. Cirilo, A.A. Boettcher, C.M. Radeke, and C.A. Vandenberg. 1999. Membrane topology of the amino-terminal region of the sulfonylurea receptor. *J. Biol. Chem.* 274:29122–29129. doi:10.1074/jbc.274.41.29122

Schwappach, B., N. Zerangue, Y.N. Jan, and L.Y. Jan. 2000. Molecular basis for K(ATP) assembly: transmembrane interactions mediate association of a K^+ channel with an ABC transporter. *Neuron.* 26:155–167. doi:10.1016/S0896-6273(00)81146-0

Shyng, S.-L., and C.G. Nichols. 1998. Membrane phospholipid control of nucleotide sensitivity of K_{ATP} channels. *Science.* 282:1138–1141. doi:10.1126/science.282.5391.1138

Shyng, S.-L., T. Ferrigni, and C.G. Nichols. 1997. Regulation of K_{ATP} channel activity by diazoxide and MgADP. Distinct functions of the two nucleotide binding folds of the sulfonylurea receptor. *J. Gen. Physiol.* 110:643–654. doi:10.1085/jgp.110.6.643

Shyng, S.-L., T. Ferrigni, J.B. Shepard, A. Nestorowicz, B. Glaser, M.A. Permutt, and C.G. Nichols. 1998. Functional analyses of novel mutations in the sulfonylurea receptor 1 associated with persistent hyperinsulinemic hypoglycemia of infancy. *Diabetes.* 47:1145–1151. doi:10.2337/diabetes.47.7.1145

Shyng, S.-L., C.A. Cukras, J. Harwood, and C.G. Nichols. 2000. Structural determinants of PIP_2 regulation of inward rectifier K_{ATP} channels. *J. Gen. Physiol.* 116:599–608. doi:10.1085/jgp.116.5.599

Simossis, V.A., and J. Heringa. 2005. PRALINE: a multiple sequence alignment toolbox that integrates homology-extended and secondary structure information. *Nucleic Acids Res.* 33:W289–294. doi:10.1093/nar/gki390

Skach, W.R., L.B. Shi, M.C. Calayag, A. Frigeri, V.R. Lingappa, and A.S. Verkman. 1994. Biogenesis and transmembrane topology of the CHIP28 water channel at the endoplasmic reticulum. *J. Cell Biol.* 125:803–815. doi:10.1083/jcb.125.4.803

Song, D.K., and F.M. Ashcroft. 2001. ATP modulation of ATP-sensitive potassium channel ATP sensitivity varies with the type of SUR subunit. *J. Biol. Chem.* 276:7143–7149. doi:10.1074/jbc.M009959200

Stansfeld, P.J., R. Hopkinson, F.M. Ashcroft, and M.S. Sansom. 2009. PIP(2)-binding site in Kir channels: definition by multiscale biomolecular simulations. *Biochemistry.* 48:10926–10933. doi:10.1021/bi9013193

Taschenberger, G., A. Mougey, S. Shen, L.B. Lester, S. LaFranchi, and S.-L. Shyng. 2002. Identification of a familial hyperinsulinism-causing mutation in the sulfonylurea receptor 1 that prevents normal trafficking and function of K_{ATP} channels. *J. Biol. Chem.* 277:17139–17146. doi:10.1074/jbc.M200363200

Tucker, S.J., F.M. Gribble, C. Zhao, S. Trapp, and F.M. Ashcroft. 1997. Truncation of Kir6.2 produces ATP-sensitive K^+ channels in the absence of the sulphonylurea receptor. *Nature.* 387:179–183. doi:10.1038/387179a0

Tusnády, G.E., E. Bakos, A. Váradi, and B. Sarkadi. 1997. Membrane topology distinguishes a subfamily of the ATP-binding cassette (ABC) transporters. *FEBS Lett.* 402:1–3. doi:10.1016/S0014-5793(96)01478-0

Xie, L.H., S.A. John, B. Ribalet, and J.N. Weiss. 2007. Activation of inwardly rectifying potassium (Kir) channels by phosphatidylinositol-4,5-bisphosphate (PIP2): interaction with other regulatory ligands. *Prog. Biophys. Mol. Biol.* 94:320–335. doi:10.1016/j.pbiomolbio.2006.04.001

Yan, F., C.W. Lin, E. Weisiger, E.A. Cartier, G. Taschenberger, and S.-L. Shyng. 2004. Sulfonylureas correct trafficking defects of ATP-sensitive potassium channels caused by mutations in the sulfonylurea receptor. *J. Biol. Chem.* 279:11096–11105. doi:10.1074/jbc.M312810200

Yan, F.F., J. Casey, and S.-L. Shyng. 2006. Sulfonylureas correct trafficking defects of disease-causing ATP-sensitive potassium channels by binding to the channel complex. *J. Biol. Chem.* 281:33403–33413. doi:10.1074/jbc.M605195200

Yan, F.F., Y.W. Lin, C. MacMullen, A. Ganguly, C.A. Stanley, and S.-L. Shyng. 2007. Congenital hyperinsulinism associated ABCC8 mutations that cause defective trafficking of ATP-sensitive K^+ channels: identification and rescue. *Diabetes.* 56:2339–2348. doi:10.2337/db07-0150

Yi, B.A., D.L. Minor Jr., Y.F. Lin, Y.N. Jan, and L.Y. Jan. 2001. Controlling potassium channel activities: interplay between the membrane and intracellular factors. *Proc. Natl. Acad. Sci. USA.* 98:11016–11023. doi:10.1073/pnas.191351798

Zerangue, N., B. Schwappach, Y.N. Jan, and L.Y. Jan. 1999. A new ER trafficking signal regulates the subunit stoichiometry of plasma membrane K(ATP) channels. *Neuron.* 22:537–548. doi:10.1016/S0896-6273(00)80708-4